



click for updates

Cite this: *RSC Adv.*, 2016, 6, 16437

## Amide-bridged terphenyl and dithienylbenzene units for semiconducting polymers†

Masahiro Akita,<sup>‡a</sup> Masahiko Saito,<sup>‡b</sup> Itaru Osaka,<sup>\*b</sup> Tomoyuki Koganezawa<sup>c</sup> and Kazuo Takimiya<sup>ab</sup>

We here describe the synthesis, characterization, and structures of new semiconducting polymers (PIQP2T and PTPQ2T) based on amide-bridged terphenyl (IQP) and dithienylbenzene (TPQ), and their performances in organic field-effect transistors (OFETs) and organic photovoltaics (OPVs). The polymers are found to have relatively wide band gaps of >2.0 eV and deep HOMO energy levels of −5.4 eV. Interestingly both the HOMO and LUMO energy levels similarly shift upward and downward, respectively, by the  $\pi$ -extension from the monomer unit to the polymer, which can be ascribed to the delocalized HOMO and LUMO along the molecular frameworks. This suggests that IQP and TPQ can be viewed as electron-neutral building units. Both polymers had similar ordering structures in the thin film despite the fact that the IQP is more sterically hindered at the end of the moiety than TPQ. This is probably due to the strong intermolecular interactions originating in the amide group. The polymers exhibited similar hole mobilities of 0.03–0.04 cm<sup>2</sup> V<sup>−1</sup> s<sup>−1</sup> in the OFET devices. Although the PCEs were modest, the OPV devices based on these polymers showed a quite high  $V_{OC}$  of 0.94 V.

Received 31st December 2015  
Accepted 27th January 2016

DOI: 10.1039/c5ra28140g

www.rsc.org/advances

### Introduction

Semiconducting polymers are an important class of materials that can be used as the active layers for organic optoelectronic devices such as transistors (OFETs), and photovoltaics (OPVs).<sup>1,2</sup> In the development of semiconducting polymers, synthetic chemists must carefully design the backbone structure to have strong intermolecular interactions and thus good ordering structures as well as suitable electronic structures.<sup>3–5</sup> Since the  $\pi$ -building unit is the most important component of the polymer that determines the ordering and electronic structures, the exploration of new  $\pi$ -building units is crucial for the materials development.

Bridged oligo-arylenes/heteroarylenes consisting of phenylene and thiophene are widely studied  $\pi$ -building units so far. Terphenyl or dithienylbenzene bridged with substituted C,<sup>6–10</sup> Si,<sup>11</sup> Ge,<sup>11,12</sup> N,<sup>13–17</sup> and olefin<sup>18,19</sup> (Fig. 1) offer good optical and electrical properties when incorporated in donor–acceptor (D–A) semiconducting polymers, where they act as donor units. Bridging of terphenyl or dithienylbenzene moieties can suppress

the distortion of the aryl–aryl linkage, which would offer rigidity and coplanarity and thus strong intermolecular interaction, in turn leading to good ordering in thin films.<sup>20</sup> The use of amide or imide containing building unit, such as diketopyrrolopyrrole (DPP),<sup>21,22</sup> isoindigo (IID),<sup>23,24</sup> thienopyrroledione (TPD),<sup>25,26</sup> bithiopheneimide (BTI),<sup>27,28</sup> and naphthalenedicarboximide (NDI)<sup>29–31</sup> (Fig. 2) in semiconducting polymers is also a promising strategy to offer strong intermolecular interaction and thus good ordering structure in thin films. Such good ordering structure in those polymers is believed to originate in the local dipole of amide and/or imide substructures,<sup>32</sup> as well as in the donor–acceptor backbone, where they act as the acceptor units.

Recently, Kim and co-workers reported on amide-bridged dithienylbenzene, 5,11-dihydrothieno[2',3':4,5]pyrido[2,3-g]thieno[3,2-c]quinoline-4,10-dione (TPQ, Fig. 3) and its copolymers.<sup>33</sup> On the other hand, Ding and co-workers reported on an isomeric structure of TPQ, namely, thieno[2',3':5,6]pyrido[3,4-g]thieno[3,2-c]

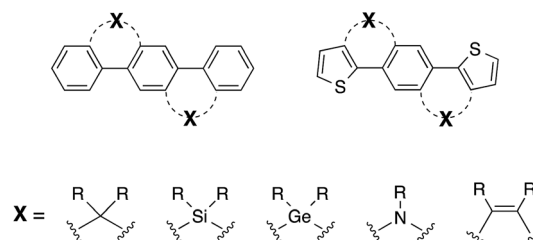


Fig. 1 Chemical structures of bridged terthiophene (left) and dithienylbenzene (right).

<sup>a</sup>Department of Applied Chemistry, Graduate School of Engineering, Hiroshima University, 1-4-1 Kagamiyama, Higashi-Hiroshima, Hiroshima 739-8527, Japan

<sup>b</sup>Emergent Molecular Function Research Group, RIKEN Center for Emergent Matter Science, Wako, Saitama 351-0198, Japan. E-mail: itaru.osaka@riken.jp

<sup>c</sup>Japan Synchrotron Radiation Research Institute (JASRI), 1-1-1 Kouto, Sayo-cho, Sayo-gun, Hyogo 679-5198, Japan

† Electronic supplementary information (ESI) available. See DOI: 10.1039/c5ra28140g

‡ These authors contributed equally.

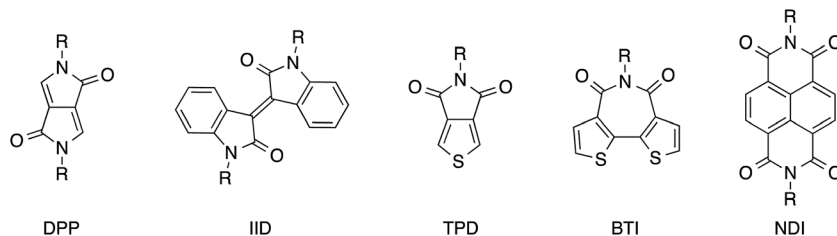


Fig. 2 Chemical structures of amide and imide-based  $\pi$ -building units.

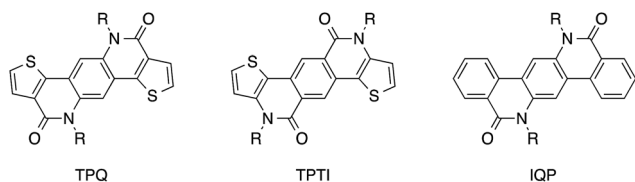


Fig. 3 Chemical structures of 5,11-dihydrothieno[2',3':4,5]pyrido[2,3-g]thieno[3,2-c]quinoline-4,10-dione (TPQ), thieno[2',3':5,6]pyrido[3,4-g]thieno[3,2-c]isoquinoline-5,11-dione (TPTI), and 6,13-dihydroisoquinolino[3,4-b]phenanthridine-5,12-dione (IQP).

isoquinoline-5,11-dione (TPTI, Fig. 3) and its copolymers.<sup>34</sup> Independently, we have also been investigating a series of amide-bridged oligoarylenes such as TPQ and 6,13-dihydroisoquinolino[3,4-*b*]phenanthridine-5,12-dione (IQP, Fig. 3) where terphenyl is the platform. Herein, we describe the synthesis of IQP and TPQ and the corresponding polymers, their properties, thin film structures, and OFET and OPV performance. It is interesting to note that, in contrast to the fact that the most of amide or imide bridged building units has strong electron deficient nature, IQP and TPQ are found to be “electron-neutral” building units<sup>35</sup> when incorporated in the  $\pi$ -conjugated polymer backbone. Although TPQ-based polymers were reported to show low field-effect mobilities of around  $10^{-5} \text{ cm}^2 \text{ V}^{-1} \text{ s}^{-1}$ ,<sup>33</sup> the TPQ-based polymer synthesized in this work exhibited mobilities as high as  $0.03 \text{ cm}^2 \text{ V}^{-1} \text{ s}^{-1}$ , which was comparable to those for the IQP-based polymer. Furthermore, the both TPQ- and IQP-based polymers were found to provide high open-circuit voltages ( $V_{\text{OC}}$ ) of 0.94 V in the OPV devices.

## Results and discussion

### Synthesis

Scheme 1 shows the synthetic route to the IQP monomer and the corresponding polymer (**PIQP2T**), where bithiophene was used as the co-unit. First, we have attempted to synthesize the IQP monomer *via* preparation of IQP (route A). **1** was reacted with 2-iodobenzoic acid methyl ester *via* the Suzuki–Miyaura cross-coupling reaction, in which the cross-coupling and cyclization were underwent sequentially in one-pot, yielding IQP. However, alkylation reaction did not afford *N,N'*-dialkyl-IQP (**2**), and instead it afforded the lactim tautomer (**3**) in a moderate yield. Similar reaction has been observed for a tetracyclic lactam compound, 4,9-dihydro-dithieno[3,2-*c*:3',2'-*h*][1,5]naphthyridine-

5,10-dione.<sup>36</sup> Therefore, we alternatively attempted to prepare a *N,N'*-dialkyl-IQP derivative *via* the route B, where the alkyl groups were introduced before the formation of the IQP moiety. 1,4-Dibromo-2,5-phenylenediboronate (**4**) was synthesized from 1,4-dibromobenzene. In the meantime, 5-bromo-2-iodobenzoyl chloride was treated with 2-decyltetradecan-1-amine to give an *N*-alkylbenzamide **5**. **4** and **5** were then cross-coupled to afford the precursor **6**, which was then cyclized *via* the Ullmann-type reaction, yielding the desired dibrominated monomer (**7**). **7** was copolymerized with distannylated bithiophene *via* the Stille coupling reaction to afford **PIQP2T**.

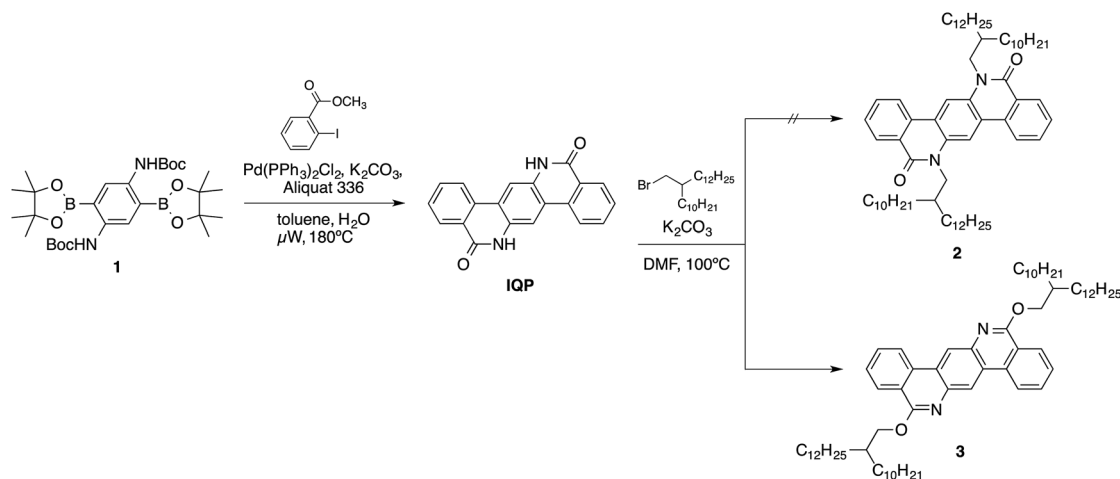
Scheme 2 depicts the synthesis of the TPQ monomer and the corresponding copolymer (**PTPQ2T**), in which the similar synthetic protocol to **PIQP2T** was used. 3-Thiophenecarboxylic acid was brominated at the 5-position, giving **8**, which was subsequently iodinated at the 2-position (**9**). **9** was converted into acid chloride and then treated with 2-decyltetradecan-1-amine to afford *N*-alkylthiophenecarboxamide **10**. **10** was cross-coupled with **4** to give **11**, which was then cyclized to yield the TPQ monomer (**12**). **12** was copolymerized with distannylated bithiophene to afford **PTPQ2T**.

Both polymers were soluble in hot chlorinated benzenes. The number average ( $M_n$ ) and weight average molecular weight ( $M_w$ ), which were determined using the gel permeation chromatography at 140 °C, were as follows:  $M_n = 21.6 \text{ kDa}$ ,  $M_w = 105.0 \text{ kDa}$  for **PIQP2T** and  $M_n = 28.0 \text{ kDa}$ ,  $M_w = 98.1 \text{ kDa}$  for **PTPQ2T** (Table 1). The relatively large polydispersity index for both the polymers is likely due to the relatively low solubility originating in the strong aggregation, which often seen in D–A semiconducting polymers.<sup>37,38</sup>

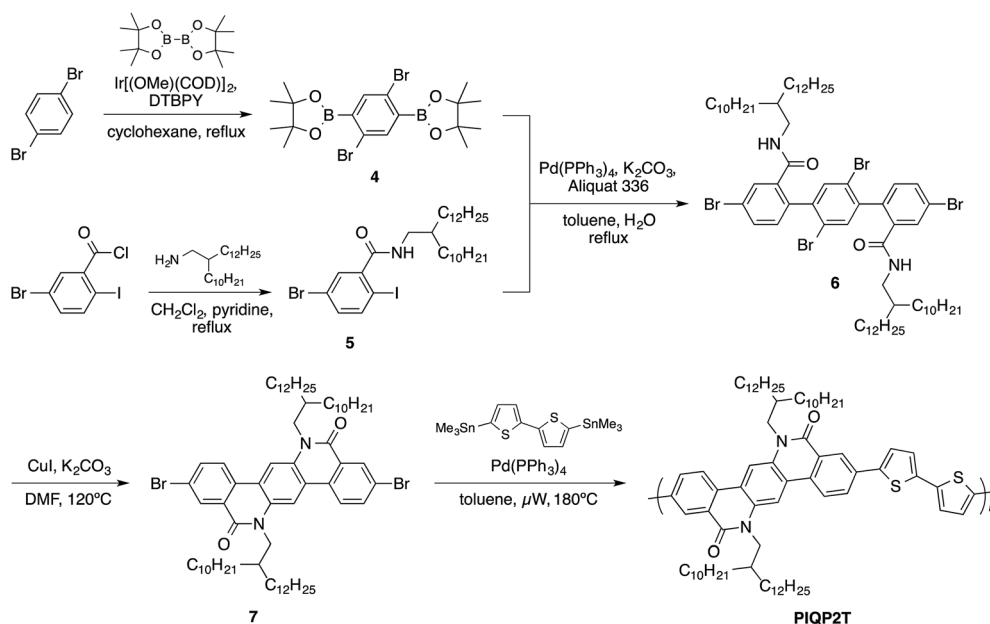
### Electronic structures

UV-vis absorption spectra of **7**, **12**, **PIQP2T**, and **PTPQ2T** in the solution are shown in Fig. 4a. While **7** afforded absorption maxima ( $\lambda_{\text{max}}$ ) at 387 nm and 407 nm, **12** afforded at 407 nm and 430 nm. This red-shift in **12** can be attributed to the enhanced coplanarity as compared to **7**, which arise from the difference of the geometry between benzene and thiophene. The optical band gap ( $E_g$ ) calculated with the absorption edge ( $\lambda_{\text{edge}}$ ), was 2.95 eV and 2.81 eV for **7** and **12**, respectively. In the polymer solution, **PIQP2T** provided a spectrum with  $\lambda_{\text{max}}$  at 490 nm and 517 nm. As similar to the monomer system, **PTPQ2T** provided a red shifted spectrum as compared to **PIQP2T**, with the  $\lambda_{\text{max}}$  at 530 nm and 565 nm. In the polymer thin film, both polymers provided  $\lambda_{\text{max}}$  similar to that in solution.  $\lambda_{\text{edge}}$  was

## Route A



## Route B

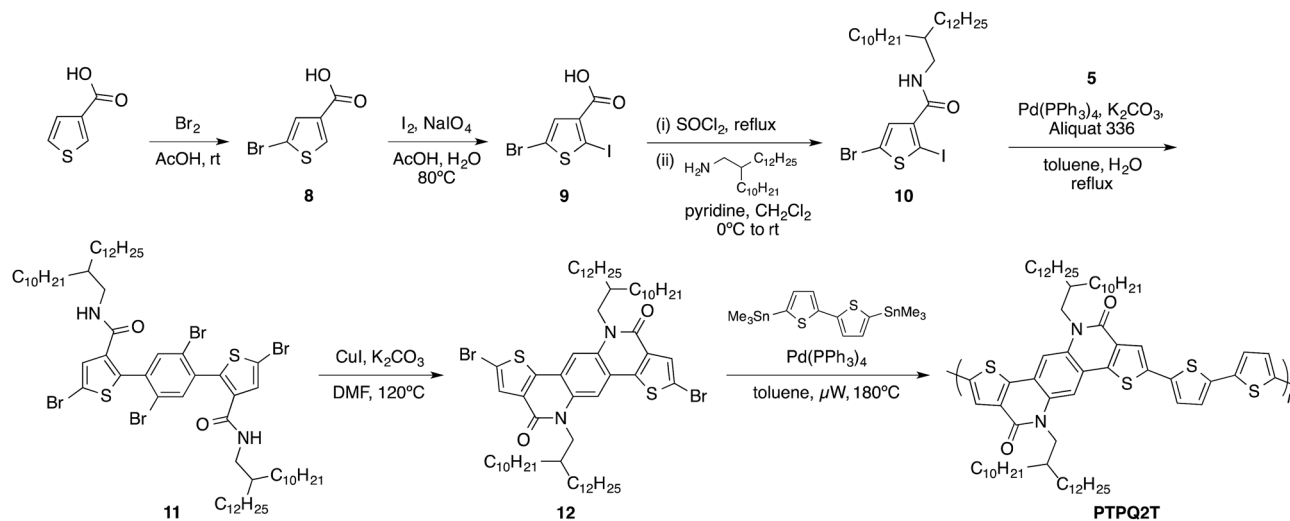


Scheme 1 Synthetic routes to the IQP moieties and the polymer.

estimated to be 550 nm and 613 nm for **PIQP2T** and **PTPQ2T**, which corresponds to  $E_g$  of 2.25 eV and 2.02 eV, respectively (Table 1).

Cyclic voltammetry (CV) was used to evaluate the highest occupied molecular orbital (HOMO) energy level ( $E_{\text{HOMO}}$ ) of the materials (Fig. 4b). While the measurement of 7 and 12 was carried out in the solution, the measurement of **PIQP2T** and **PTPQ2T** was carried out in the thin film. The onset oxidation potentials of 7 and 12 against Ag/AgCl were 1.34 V and 1.38 V, which correspond to  $E_{\text{HOMO}}$ s of  $-5.70$  eV and  $-5.74$  eV, respectively. The lowest unoccupied molecular orbital (LUMO) energy level ( $E_{\text{LUMO}}$ ), estimated by the addition of  $E_g$  to  $E_{\text{HOMO}}$ , were  $-2.75$  eV and  $-2.93$  eV for 7 and 12, respectively. This means that TPQ has relatively higher electron affinity than IQP, and the difference in  $E_g$  mostly arise from the difference in  $E_{\text{LUMO}}$ . The onset oxidation potentials

of **PIQP2T** and **PTPQ2T** were 1.02 V and 1.07 V, with which  $E_{\text{HOMO}}$ s were determined to be  $-5.38$  eV and  $-5.43$  eV, respectively.  $E_{\text{LUMO}}$ s of **PIQP2T** and **PTPQ2T** were estimated to be  $-3.13$  eV and  $-3.41$  eV, respectively. As a result, in these systems,  $E_{\text{HOMO}}$  and  $E_{\text{LUMO}}$  shifted upward and downward, respectively, by the polymerization (extension of  $\pi$ -conjugation along the backbone), which is similar to the case in TPD and thiazolothiazole polymer systems.<sup>39</sup> With such variation of the  $E_{\text{HOMO}}$  and  $E_{\text{LUMO}}$  between the monomers and polymers and the fact that the  $E_{\text{HOMO}}$  and  $E_{\text{LUMO}}$  were not so shallow and deep, respectively, the IQP and TPQ units can be regarded as “electron-neutral” building units.<sup>35</sup> Such perturbation of  $E_{\text{HOMO}}$  and  $E_{\text{LUMO}}$  probably due to the fact that both HOMOs and LUMOs are well-delocalized along the backbone (Fig. 4c).



Scheme 2 Synthesis of the TPQ-based polymer.

Table 1 Chemical, physicochemical, and optical properties of the polymers

Polymer	$M_n^a$ (kDa)	$M_w^a$ (kDa)	PDI <sup>a</sup>	$\lambda_{\max}^b$ (nm)	$E_g^c$ (eV)	$E_{\text{HOMO}}^d$ (eV)	$E_{\text{LUMO}}^e$ (eV)
PIQP2T	21.6	105.0	4.9	490, 517	2.25	-5.38	-3.13
PTPQ2T	28.0	98.1	3.5	530, 565	2.02	-5.43	-3.41

<sup>a</sup> Determined by GPC using polystyrene standard and DCB as the eluent at 140 °C. <sup>b</sup> Absorption maxima in the thin film. <sup>c</sup> Optical bandgaps determined from the absorption onset. <sup>d</sup> HOMO energy levels evaluated by cyclic voltammetry. <sup>e</sup> LUMO energy levels determined by adding the optical bandgap to the HOMO energy level.

### OFET properties

OFET devices with **PIQP2T** and **PTPQ2T** were fabricated and evaluated by using a bottom gate top contact architecture. *1H,1H,2H,2H*-Perfluorodecyltriethoxysilane (FDTS) was used as the self-assembled monolayer (SAM) on top of the SiO<sub>2</sub>/Si substrate, on which the polymer solution in *o*-dichlorobenzene (DCB) was spun and then the resulting thin films were annealed at 150 °C for 30 minutes. Both polymers demonstrated p-channel behavior. Fig. 5 shows the typical transfer and output curves of the OFETs, in which the transfer characteristics were obtained with the drain voltage ( $V_D$ ) of -60 V. Although the output curves showed a slight non-linear behavior at the low  $V_D$  region, they gave fairly good saturation behavior at the higher  $V_D$  region. The hole mobilities extracted from the saturation region were similar for both polymers. The highest hole mobility was 0.037 and 0.027 cm<sup>2</sup> V<sup>-1</sup> s<sup>-1</sup> for **PIQP2T** and **PTPQ2T**, respectively, and the current on/off ratios were as high as 10<sup>6</sup> (Table 2).

### OPV properties

OPV cells were fabricated using an inverted architecture with ZnO as the electron transport layer and MoO<sub>3</sub> as the hole transport layer. The polymer/[6,6]-phenyl-C<sub>71</sub>-butyric acid methyl ester (PC<sub>71</sub>BM) solution in DCB with 3 volume% of 1,8-diodooctane (DIO) was spin-coated to form bulk heterojunction thin films. Fig. 6 displays the external quantum efficiency

spectra and current density-voltage curves of the devices. The photovoltaic parameters are summarized in Table 2. Both the **PIQP2T** and **PTPQ2T**-based cells showed the photoresponse up to slightly longer wavelength region than  $\lambda_{\text{edge}}$  of the polymer absorption spectra. Whereas  $\lambda_{\text{edge}}$  for **PIQP2T** and **PTPQ2T** was 550 nm and 613 nm, respectively, as described above, the photoresponse reaches over 700 nm for both the cells (Fig. 6a). The photoresponse at longer wavelength region such as 550–700 nm likely comes from PC<sub>61</sub>BM. The EQE was around 40–45% at the region of  $\lambda_{\text{max}}$  for both the cells, which reflect the modest short-circuit currents ( $J_{\text{SCS}}$ ) (Fig. 6b, Table 2). Again, similar power conversion efficiencies (PCEs) such as 2.3% (**PIQP2T**) and 2.7% (**PTPQ2T**) were obtained for these polymer cells. It should be noted that although the overall PCEs were not so high, fairly high  $V_{\text{OCs}}$  of 0.94 V was obtained for both cells. This is consistent with the relatively deep  $E_{\text{HOMO}}$  of the polymers. The relatively wide band gap and the very high  $V_{\text{OC}}$  could be advantageous for the use as the front cell in tandem architecture.<sup>40,41</sup>

### Thin film structure and morphology

The ordering structure of the polymers and polymer/PC<sub>71</sub>BM blend films were investigated by the grazing incidence X-ray diffraction (GIXD) measurements. Fig. 7a and c displays the two-dimensional (2D) GIXD patterns of the polymer neat film for **PIQP2T** and **PTPQ2T**, respectively. Both the polymers gave

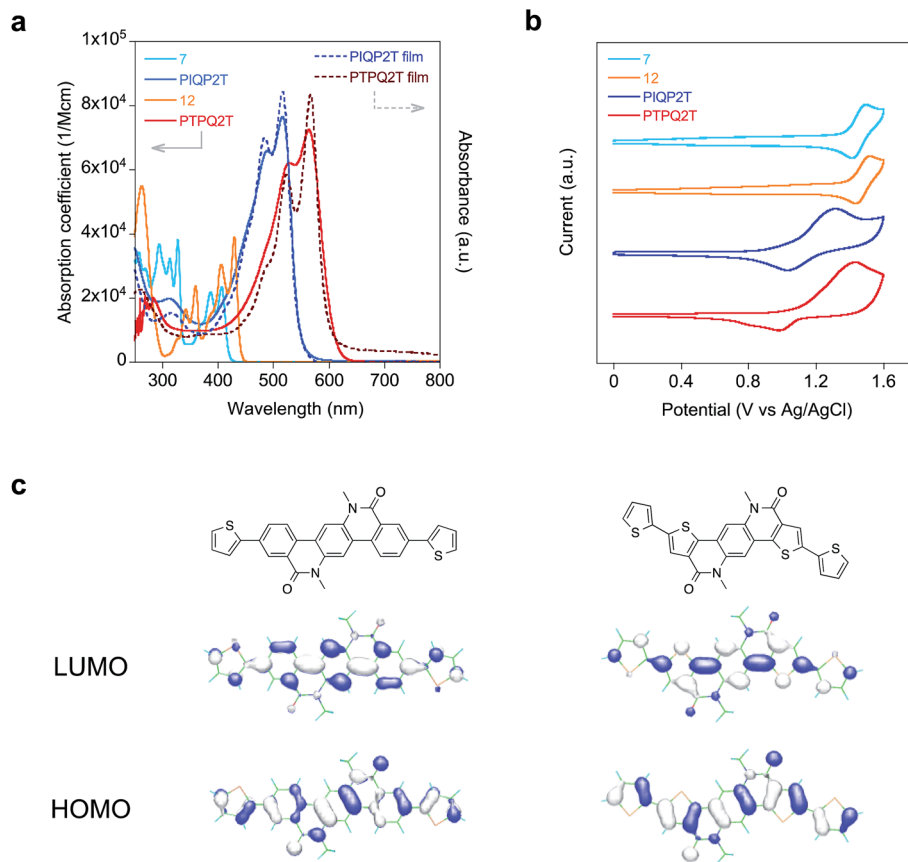


Fig. 4 (a) UV-vis absorption spectra in the solution (solid lines) and in the film (dot lines). (b) Cyclic voltammograms. **7** and **12** were measured in benzonitril solution, and PIQP2T and PTPQ2T were measured in thin film. (c) HOMO and LUMO geometries calculated by the DFT method at the B3LYP/6-31 g (d) level.

diffractions corresponding to the lamellar structure and the  $\pi$ - $\pi$  stacking structure along the  $q_z$  and  $q_{xy}$  axes, respectively, indicating the edge-on orientation (Fig. 7a and c). Fig. 7e and f shows the cross sectional profiles of the patterns along the  $q_z$  and  $q_{xy}$  axes, respectively. It is interesting to note that the  $\pi$ - $\pi$  stacking peaks of both PIQP2T and PTPQ2T appeared at  $q_{xy} = 1.71 \text{ \AA}^{-1}$  (indicated by arrows), which corresponds to a distance

of *ca.*  $3.7 \text{ \AA}$ . In general, thiophene-thiophene linkage (TPQ-thiophene) provide smaller dihedral angle than benzene-thiophene linkage (IQP-thiophene), and thus is expected to give better ordering structure. However, it was found that the ordering structures of PIQP2T and PTPQ2T were fairly similar. This is probably as a result of strong intermolecular interaction originating in the amide moiety having a local dipole, which

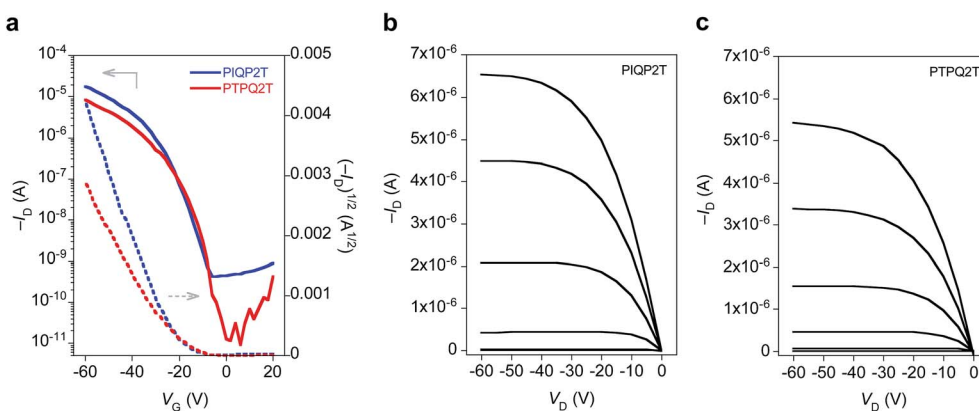


Fig. 5 Transfer (a) and output (b, c) curves of the OFETs. (b) PIQP2T, (c) PTPQ2T. Transfer curves were obtained with the drain voltage ( $V_D$ ) of  $-60 \text{ V}$ .

Table 2 OFET and OPV properties of the polymer-based devices

Polymer	OFET			OPV			
	$\mu^a$ ( $\text{cm}^2 \text{V}^{-1} \text{s}^{-1}$ )	$V_T^b$ (V)	$I_{\text{on}}/I_{\text{off}}^c$	$J_{\text{SC}}$ ( $\text{mA cm}^{-2}$ )	$V_{\text{OC}}$ (V)	FF	PCE (%)
PIQP2T	0.037	-19.6	$10^6$	4.7	0.94	0.50	2.3
PTPQ2T	0.027	-23.0	$10^6$	5.6	0.94	0.51	2.7

<sup>a</sup> Hole mobilities evaluated at the saturation region. <sup>b</sup> Threshold voltages. <sup>c</sup> Current on and off ratios.

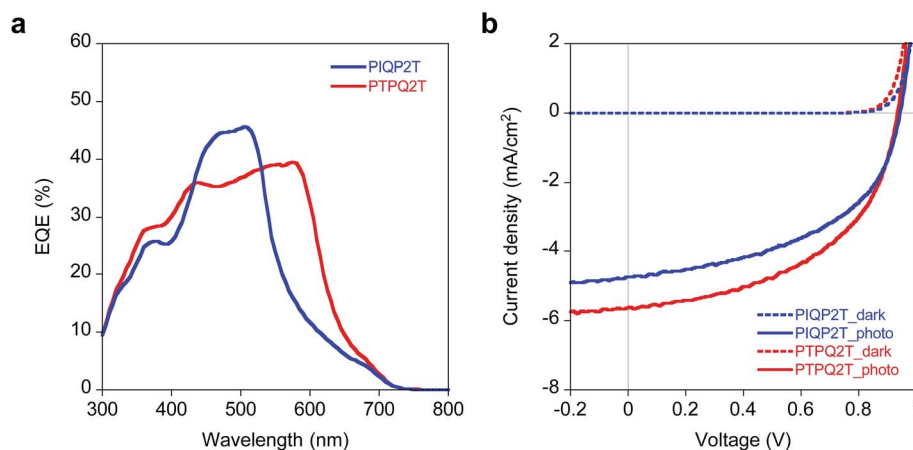


Fig. 6 EQE spectra (a) and  $J$ - $V$  curves (b) of the OPV cells using PIQP2T and PTPQ2T combined with PC<sub>71</sub>BM.

reduces the difference of the steric effect. These results agree well with the charge transport property observed in OFETs. In the blend film (Fig. 7b and d), both PIQP2T and PTPQ2T gave similar patterns to the neat film, *i.e.*, the backbone orientation was preserved. The  $\pi$ - $\pi$  stacking distance was also almost the same as in the neat film. The unfavorable orientation for OPV devices seen in the blend film could be one of the limiting factors for the OPV performance. Nevertheless, further modification of the molecular structure can realize the favorable face-on orientation, which possibly enhances the OPV performance.

## Conclusion

We have synthesized new semiconducting polymers (PIQP2T and PTPQ2T) based on amide-bridged terphenyl (IQP) and dithienylbenzene (TPQ) building units. These polymers had relatively wide band gap of  $>2.0$  eV with deep  $E_{\text{HOMO}}$ s of  $-5.4$  eV.  $E_{\text{HOMO}}$  and  $E_{\text{LUMO}}$  similarly shifted upward and downward, respectively, by the  $\pi$ -extension from the monomer unit to the polymer, which can be ascribed to the delocalized HOMO and LUMO along the frameworks. These results imply that IQP and TPQ can be viewed as electron-neutral building units.<sup>35</sup> The polymers presented here exhibited similar hole mobilities of  $0.03$ – $0.04$   $\text{cm}^2 \text{V}^{-1} \text{s}^{-1}$  in the OFET devices. Although the PCEs were modest, the OPV devices based on these polymers showed quite high  $V_{\text{OC}}$  of  $0.94$  V, which reflects deep  $E_{\text{HOMO}}$ s of  $-5.4$  eV. Interestingly, both polymers had similar ordering structures in the thin film despite that the IQP is likely to be more sterically hindered at the end of the moiety than TPQ. This is probably

due to the strong intermolecular interactions originating in the amide group. With these aspects, IQP and TPQ can be useful  $\pi$ -building units for semiconducting polymers.

## Experimental section

### Synthesis

All chemicals and solvents are of reagent grade unless otherwise indicated. THF, toluene, cyclohexane, and DMF were purified by a Glass Contour Solvent System (Nikko Hansen & Co., Ltd.) prior to use. **1** was synthesized according to the literature procedure.<sup>42</sup> Polymerization was carried out with a microwave reactor (Biotage Initiator). Nuclear magnetic resonance (NMR) spectra were obtained in deuterated chloroform and DCB with TMS as internal reference by using a JNM-ECS400 (JEOL RESONANCE). Molecular weights were determined by gel permeation chromatography (GPC) by calibrating with polystyrene standards using a TOSOH HLC-8121GPC/HT at  $140$  °C with DCB as the solvent.

**Isouquinolino[3,4-*b*]phenanthridine-5,12(6*H*,13*H*)-dione (IQP).** **2** (100 mg, 1.8 mmol), methyl 2-bromobenzoate (92.1 mg, 4.46 mmol), Pd(PPh<sub>3</sub>)<sub>4</sub> (1.4 mg, 0.0012 mol), 1.0 mL of 1 M K<sub>2</sub>CO<sub>3</sub> aq, 1 drop of aliquat 336, and 5 mL of toluene were added to a vial. The vial was then purged with argon and sealed. The sealed vial was heated at  $130$  °C for 5 hour in a microwave reactor. After cooling to room temperature, the reaction mixture was filtered and the residue was washed with acetone to give the desired compound as yellow solid (34.0 mg, 62%). HRMS: calcd for C<sub>20</sub>H<sub>13</sub>O<sub>2</sub>N<sub>2</sub>: [M +

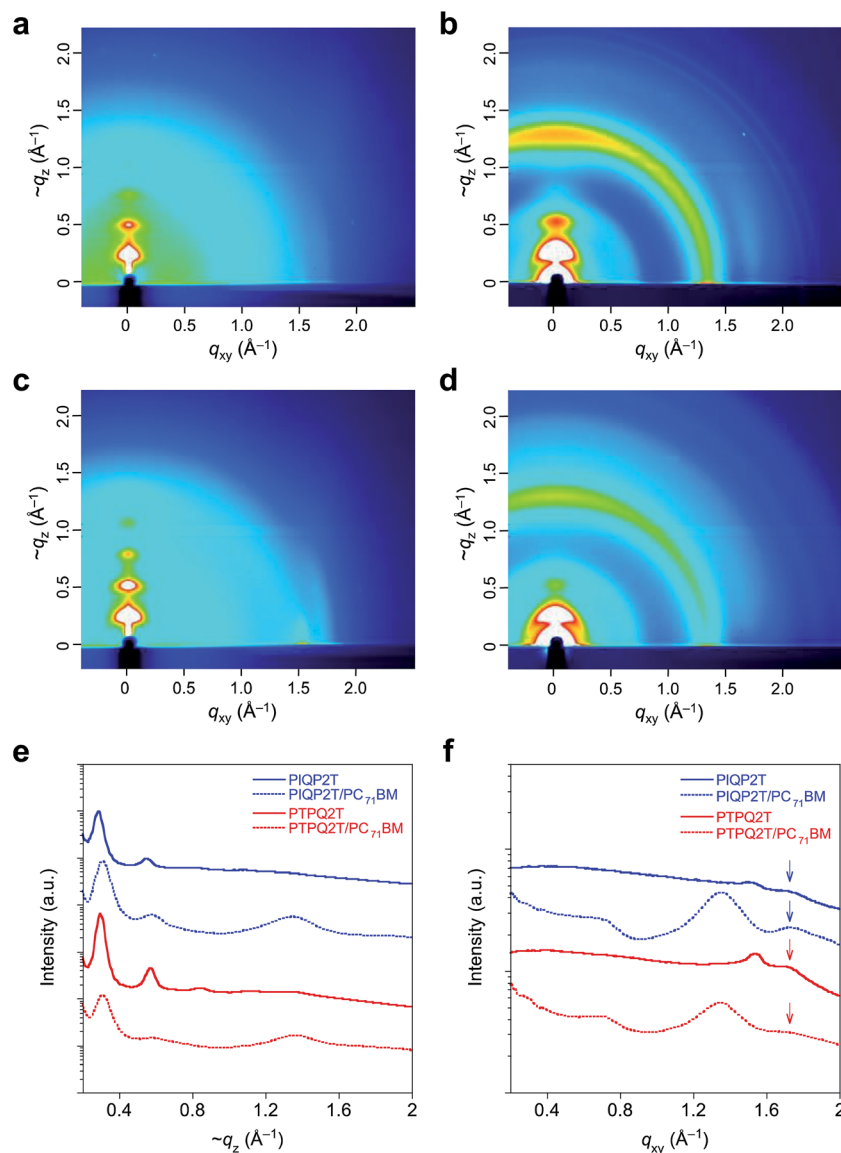


Fig. 7 2D GIXD patterns (a–d) and cross sectional profiles along the  $q_z$  (e) and  $q_{xy}$  (f) axes. (a) PIQP2T neat film, (b) PIQP2T/PC<sub>71</sub>BM blend film (1 : 2), (c) PTPQ2T neat film, (d) PTPQ2T/PC<sub>71</sub>BM blend film (1 : 2). The arrows in Fig. 6f show the  $\pi$ - $\pi$  stacking peaks.

$H^+$ : 313.09715. Found: 313.09732. NMR not available due to the insolubility.

**5,12-Bis((2-decyltetradecyl)oxy)isoquinolino[3,4-*b*]phenanthridine (3).** IQP (50.0 mg, 0.16 mmol), 1-bromo-2-decyltetradecane (267 mg, 0.64 mmol), and K<sub>2</sub>CO<sub>3</sub> (88.0 g, 0.64 mmol) were added in 5 mL of DMF. The mixture was stirred at 100 °C for 12 hours. The reaction mixture was then cooled to room temperature, and then filtered through Celite. After the solvent was removed, the residue was purified by column chromatography on silica gel eluted with chloroform/hexane (1 : 2), giving 3 (not 2) as colorless oil (30.0 mg, 19%). HRMS calcd for C<sub>68</sub>H<sub>109</sub>N<sub>2</sub>O<sub>2</sub> [M + H]<sup>+</sup>: 985.84890. Found: 985.84887. <sup>1</sup>H NMR (400 MHz, CDCl<sub>3</sub>):  $\delta$  8.81 (s, 2H), 8.54 (d, 2H,  $J$  = 8.4 Hz), 8.49 (d, 2H,  $J$  = 8.4 Hz), 7.95 (dd, 2H,  $J$  = 7.3 Hz), 7.93 (dd, 2H,  $J$  = 7.5 Hz), 4.60 (d, 4H,  $J$  = 5.4 Hz), 3.72 (m, 2H), 1.63–1.24 (m, 48H), 0.88 (t, 6H,  $J$  = 7.2 Hz). <sup>13</sup>C NMR (100 MHz, CDCl<sub>3</sub>):

140.2, 134.3, 128.0, 124.5, 123.5, 122.3, 122.1, 120.5, 69.6, 37.8, 32.0, 31.9, 30.2, 29.9, 29.5, 27.1, 22.8, 14.3.

**2,2'-(2,5-Dibromo-1,4-phenylene)bis(4,4,5,5-tetramethyl-1,3,2-dioxaborolane) (4).** A mixture of (1,5-cyclooctadiene) (methoxy) iridium(i) (116 mg, 0.17 mmol), 4,4'-di-*tert*-butyl-2,2'-dipyridyl (110 mg, 0.40 mmol) in 150 mL of cyclohexane was refluxed for 30 minutes, after which bis(pinacolato)diboron (11.8 g, 46.6 mmol) was added and the mixture was refluxed for 30 minutes. 1,4-Dibromobenzene (5.00 g, 21.2 mmol) was then added and the mixture was refluxed for 12 hours. After cooling to room temperature, water was added and the aqueous layer was extracted with chloroform. The organic layer was washed with water and brine, and then dried over anhydrous MgSO<sub>4</sub>. The solvent was removed, and the residue was washed with cold methanol to give the desired compound as white solid (6.88 g, 67%). HRMS: calcd for C<sub>18</sub>H<sub>27</sub>O<sub>4</sub>B<sub>2</sub>Br<sub>2</sub> [M + H]<sup>+</sup>: 487.04567.

Found: 487.04532.  $^1\text{H}$  NMR (400 MHz,  $\text{CDCl}_3$ ):  $\delta$  7.74 (s, 2H), 1.37 (s, 24H).  $^{13}\text{C}$  NMR (100 MHz,  $\text{CDCl}_3$ ):  $\delta$  140.3, 126.5, 85.0, 25.1.

**5-Bromo-*N*-(2-decyltetradecyl)-2-iodobenzene (5).** To a solution of 2-decyltetradecylamine (7.00 g, 19.8 mmol) in 30 mL of pyridine was added 5-bromo-2-iodobenzoyl chloride (5.80 g, 16.8 mmol) in 20 mL of dichloromethane at 0 °C. After the solution was stirred at 0 °C for 30 minutes and then at room temperature for 2 hours, 150 mL of 2 M HCl aq and 100 mL of dichloromethane were added. The organic layer was washed twice with 100 mL of brine and dried over  $\text{MgSO}_4$ . After the solvent was removed, the residue was purified by column chromatography on silica gel with chloroform to give the desired compound as white solid (3.54 g, 70%). HRMS calcd for  $\text{C}_{31}\text{H}_{54}\text{ONBrI}$  [ $\text{M} + \text{H}$ ] $^+$ : 662.24280. Found: 662.24274.  $^1\text{H}$  NMR (400 MHz,  $\text{CDCl}_3$ ):  $\delta$  7.69 (d, 1H,  $J = 6.8$  Hz), 7.50 (d, 1H,  $J = 1.6$  Hz), 7.23 (dd, 1H,  $J = 6.8$  Hz,  $J = 1.5$  Hz), 5.70 (s, 1H), 3.39 (dd, 2H,  $J = 4.7$  Hz), 1.40–1.20 (m, 40H), 0.88 (t, 6H,  $J = 5.3$  Hz).  $^{13}\text{C}$  NMR (100 MHz,  $\text{CDCl}_3$ ):  $\delta$  168.3, 144.7, 141.5, 134.4, 1331.6, 123.0, 90.7, 43.7, 38.2, 32.3, 30.3, 30.0, 27.0, 23.1, 14.5.

**2',4,4'',5'-Tetrabromo-*N,N''*-bis(2-decyltetradecyl)-(1,1':4',1''-terphenyl)-2,2''-dicarboxamide (6).** **4** (0.90 g, 1.84 mmol), **5** (2.50 g, 3.77 mmol), and 15 mL of 2 M  $\text{K}_2\text{CO}_3$  aq were added in 30 mL of toluene, which was purged with  $\text{N}_2$  for 30 minutes.  $\text{Pd}(\text{PPh}_3)_4$  (0.11 mg, 0.09 mmol) and 1 drop of Aliquat 336 was then added, and the reaction mixture was refluxed for 15 hours. After cooling to room temperature, water was added and the aqueous layer was extracted with dichloromethane. The organic layer was washed with water and brine, and then dried over anhydrous  $\text{MgSO}_4$ . The solvent was removed and the residue was purified by column chromatography on silica gel with chloroform, and was further purified with preparative GPC using chloroform as the eluent to give the desired compound as white solid (1.28 g, 53%). HRMS calcd for  $\text{C}_{68}\text{H}_{109}\text{O}_2\text{N}_2\text{Br}_4$  [ $\text{M} + \text{H}$ ] $^+$ : 1301.52171. Found: 1301.52368.  $^1\text{H}$  NMR (400 MHz,  $\text{CDCl}_3$ ):  $\delta$  7.83 (d, 2H,  $J = 1.8$  Hz), 7.64 (dd, 2H,  $J = 8.0$  Hz), 7.57 (s, 2H), 7.11 (dd, 2H,  $J = 8.2$  Hz), 5.50 (s, 2H), 3.22 (m, 4H), 1.50–1.20 (m, 80H), 0.90–0.84 (m, 12H).  $^{13}\text{C}$  NMR (100 MHz,  $\text{CDCl}_3$ ):  $\delta$  167.2, 142.2, 138.3, 136.0, 134.8, 133.3, 132.5, 131.6, 123.3, 122.3, 42.9, 38.1, 32.3, 32.1, 30.3, 30.0, 30.0, 29.7, 29.7, 27.0, 23.1, 14.5.

**3,10-Dibromo-6,13-bis(2-decyltetradecyl)-6,13-dihydroisoquinolino[3,4-*b*]phenanthridine-5,12-dione (7).** **6** (1.00 g, 0.77 mmol)  $\text{CuI}(\text{i})$  (0.073 mg, 0.38 mmol), and  $\text{K}_2\text{CO}_3$  (0.26 mg, 1.91 mmol) were added in 30 mL of DMF. The mixture was stirred at 120 °C for 12 hours. After cooling to room temperature, water was added and the aqueous layer was extracted with chloroform. The organic layer was washed with water and brine, and then dried over anhydrous  $\text{MgSO}_4$ . The solvent was removed and the residue was purified by column chromatography on silica gel with hexane/chloroform (1 : 1), and then was recrystallized with ethyl acetate/acetone to give the desired compound as yellow solid (0.87 g, 99%). HRMS calcd for  $\text{C}_{68}\text{H}_{107}\text{O}_2\text{N}_2\text{Br}_2$  [ $\text{M} + \text{H}$ ] $^+$ : 1141.66938. Found: 1141.67078.  $^1\text{H}$  NMR (400 MHz,  $\text{CDCl}_3$ ):  $\delta$  8.75 (dd, 2H), 8.17 (s, 2H), 8.09 (dd, 2H,  $J = 8.6$  Hz), 7.88 (dd, 2H,  $J = 8.6$  Hz), 4.50 (s, 4H), 2.07 (s, 2H), 1.50–1.20 (m, 80H), 0.90–0.86 (m, 12H).  $^{13}\text{C}$  NMR (100 MHz,  $\text{CDCl}_3$ ):  $\delta$  160.5,

136.0, 132.9, 132.6, 131.7, 127.8, 123.5, 123.5, 120.6, 109.8, 46.7, 37.1, 32.3, 32.2, 30.4, 30.1, 30.0, 30.0, 29.7, 27.6, 23.0, 14.5.

**5-Bromothiophene-3-carboxylic acid (8).** To a solution of thiophene-3-carboxylic acid (2.00 g, mmol) in 20 mL of acetic acid was added bromine (2.49 g, 15.6 mmol). The mixture was stirred at room temperature for 30 minutes, and then water was added. The precipitate was filtered and recrystallized with hot water to give the desired compound as white solid (1.42 g, 44%). HRMS calcd for  $\text{C}_5\text{H}_2\text{O}_2\text{BrNa}_2\text{S}$  [ $\text{M} - \text{H} + 2\text{Na}$ ] $^+$ : 250.87488. Found: 250.87491.  $^1\text{H}$  NMR (400 MHz,  $\text{CDCl}_3$ ):  $\delta$  8.11 (s, 1H), 7.51 (s, 1H).  $^{13}\text{C}$  NMR (100 MHz,  $\text{CDCl}_3$ ):  $\delta$  167.3, 136.2, 133.4, 130.7, 113.7.

**5-Bromo-2-iodothiophene-3-carboxylic acid (9).** **8** (1.00 g, 4.83 mmol), periodic acid (0.33 g, 1.45 mmol), and iodine (0.98 g, 3.86 mmol) was added to 30 mL of acetic acid and 15 mL of water. The mixture was stirred at 80 °C for 9 hours. After cooling to room temperature,  $\text{Na}_2\text{S}_2\text{O}_3$  aq was added and the resulting precipitate was filtered. The residue was washed with water and dried *in vacuo* to give the desired compound as white solid (1.38 g, 86%). HRMS calcd for  $\text{C}_5\text{HO}_2\text{BrINa}_2\text{S}$  [ $\text{M} - \text{H} + 2\text{Na}$ ] $^+$ : 376.77152. Found: 376.77164.  $^1\text{H}$  NMR (400 MHz,  $\text{CDCl}_3$ ):  $\delta$  7.36 (s, 1H).  $^{13}\text{C}$  NMR (100 MHz,  $\text{CDCl}_3$ ):  $\delta$  162.2, 142.5, 132.0, 116.9, 74.3.

**5-Bromo-*N*-(2-decyltetradecyl)-2-iodothiophene-3-carboxamide (10).** To a solution of **9** (2.17 g, 10.5 mmol) in 20 mL of dichloromethane was added 20 mL of thionyl chloride, and the solution was refluxed for 3 hours. The solution was then added to a solution of 2-decyltetradecyl (4.45 g, 12.6 mmol) in 30 mL of pyridine at 0 °C. The reaction solution was stirred at 0 °C for 30 minutes and then at room temperature for 3 hours. 100 mL of 2 M HCl aq and 100 mL of dichloromethane were added and the extracted organic layer was washed twice with 100 mL of brine and dried over  $\text{MgSO}_4$ . After the solvent was removed, the residue was purified by column chromatography on silica gel with chloroform to give the desired compound as white solid (4.75 g, 68%). HRMS calcd for  $\text{C}_{29}\text{H}_{51}\text{ONBrINaS}$  [ $\text{M} + \text{Na}$ ] $^+$ : 690.18116. Found: 690.18085.  $^1\text{H}$  NMR (400 MHz,  $\text{CDCl}_3$ ):  $\delta$  7.73 (s, 2H), 7.37 (s, 2H), 5.4 (s, 2H), 3.24 (m, 4H), 1.41 (m, 2H), 1.30–1.00 (m, 80H), 0.90–0.86 (m, 12H).  $^{13}\text{C}$  NMR (100 MHz,  $\text{CDCl}_3$ ):  $\delta$  162.2, 142.5, 132.0, 117.0, 74.3, 43.4, 38.1, 32.3, 30.3, 30.0, 30.0, 30.0, 29.7, 27.0, 23.1.

**2,2'-(2,5-Dibromo-1,4-phenylene)bis(5-bromo-*N*-(2-decyltetradecyl)thiophene-3-carboxamide) (11).** **5** (0.51 g, 1.03 mmol), **11** (1.53 g, 2.27 mmol), and 5 mL of 2 M  $\text{K}_2\text{CO}_3$  aq were added in 16 mL of toluene, which was purged with  $\text{N}_2$  for 30 minutes.  $\text{Pd}(\text{PPh}_3)_4$  (60.0 mg, 0.05 mmol) and 1 drop of Aliquat 336 were added, and the mixture was refluxed for 15 hours. After cooling to room temperature, water was added and the aqueous layer was extracted with dichloromethane. The organic layer was washed with water and brine, and then dried over anhydrous  $\text{MgSO}_4$ . The solvent was removed and the residue was purified by column chromatography on silica gel with hexane/chloroform (1 : 1), and was further purified with preparative GPC using chloroform as the eluent to give the desired compound as white solid (0.163 g, 12%). HRMS calcd for  $\text{C}_{64}\text{H}_{105}\text{Br}_4\text{N}_2\text{O}_2\text{S}_2$  [ $\text{M} + \text{H}$ ] $^+$ : 1313.43455. Found: 1313.43652.  $^1\text{H}$  NMR (400 MHz,  $\text{CDCl}_3$ ):  $\delta$  7.73 (d, 2H), 7.37 (d, 2H), 5.40 (s, 2H), 3.24 (d, 2H), 1.41–0.95 (m, 82H), 0.90–0.86 (m, 12H).  $^{13}\text{C}$  NMR

(100 MHz, CDCl<sub>3</sub>):  $\delta$  162.2, 140.9, 136.9, 136.5, 136.3, 130.8, 124.1, 113.9, 42.7, 37.7, 32.3, 32.2, 30.4, 30.1, 30.0, 30.0, 29.7, 27.0, 23.1, 14.5.

**2,8-Dibromo-5,11-bis(2-decyltetradecyl)thieno[2',3':4,5]pyridido[2,3-g]thieno[3,2-c]quinoline-4,10-dione (12).** **11** (100 mg, 0.076 mmol), CuI(I) (8.0 mg, 0.038 mmol), and K<sub>2</sub>CO<sub>3</sub> (21.0 mg, 0.15 mmol) were added to 10 mL of DMF. The mixture was stirred at 120 °C for 12 hours. After cooling to room temperature, water was added and the aqueous layer was extracted with chloroform. The organic layer was washed with water and brine, and then dried over anhydrous MgSO<sub>4</sub>. The solvent was removed and the residue was purified by column chromatography on silica gel with hexane/chloroform (1 : 1) and by preparative GPC using chloroform as the eluent, and then recrystallized with ethyl acetate/chloroform to give the desired compound as yellow solid (0.062 mg, 82%). HRMS calcd for C<sub>64</sub>H<sub>103</sub>Br<sub>2</sub>N<sub>2</sub>O<sub>2</sub>S<sub>2</sub> [M + H]<sup>+</sup>: 1153.58222. Found: 1153.58350. <sup>1</sup>H NMR (400 MHz, CDCl<sub>3</sub>):  $\delta$  7.73 (s, 2H), 7.59 (s, 2H), 4.36 (m, 4H), 1.98 (m, 2H), 2.00 (m, 4H), 1.50–1.20 (m, 80H), 0.90–0.86 (m, 12H). <sup>13</sup>C NMR (100 MHz, CDCl<sub>3</sub>):  $\delta$  157.6, 145.5, 132.6, 132.5, 130.2, 118.9, 114.5, 110.3, 46.5, 37.1, 32.3, 30.5, 30.0, 29.7, 27.5, 23.1, 14.5.

**PIQP2T. 8** (57.2 mg, 0.05 mmol), 5,5'-bis(trimethylstannyl)-2,2'-bithiophene (24.6 mg, 0.05 mmol), Pd(PPh<sub>3</sub>)<sub>4</sub> (2.31 mg, 2.0  $\mu$ mol), and 2 mL of toluene were added to a vial. The vial was then purged with Ar and sealed. The sealed vial was heated 180 °C for 40 min using a microwave reactor. After cooling to room temperature, the reaction mixture was precipitated into 100 mL of methanol containing 5 mL of concentrated HCl, and stirred at room temperature for 6 hours. The precipitate was filtered and subjected to soxhlet extraction with methanol and hexane to remove low molecular weight fraction. The residue was washed out with chloroform, which was concentrated and precipitated into methanol. The precipitate was filtered to give the polymer as dark orange solid (60.0 mg, 98%). Anal. calcd for C<sub>68</sub>H<sub>107</sub>O<sub>2</sub>N<sub>2</sub>: C, 74.43; H, 9.37; N, 2.41. Found: C, 74.20; H, 9.21; N, 2.36. GPC (DCB, 140 °C):  $M_n$  = 21.6 kDa,  $M_w$  = 105.0 kDa, PDI = 4.9.

**PTPQ2T. 13** (57.8 mg, 0.05 mmol), 5,5'-bis(trimethylstannyl)-2,2'-bithiophene (24.6 mg, 0.05 mmol), Pd(PPh<sub>3</sub>)<sub>4</sub> (2.31 mg, 2.0  $\mu$ mol), and 2 mL of toluene were added to a vial. The vial was then purged with Ar and sealed. The sealed vial was heated 180 °C for 40 min using a microwave reactor. After cooling to room temperature, the reaction mixture was precipitated into 100 mL of methanol containing 5 mL of concentrated HCl, and stirred at room temperature for 6 hours. The precipitate was filtered and subjected to soxhlet extraction with methanol, hexane, and chloroform to remove low molecular weight fraction. The residue was washed out with chlorobenzene, which was concentrated and precipitated into methanol. The precipitate was filtered to give the polymer as dark red solid (34.0 mg, 59%). Anal. calcd for C<sub>82</sub>H<sub>113</sub>N<sub>6</sub>S<sub>2</sub>: C, 79.39; H, 9.82; N, 2.44. Found: GPC (DCB, 140 °C):  $M_n$  = 28.0 kDa,  $M_w$  = 98.1 kDa, PDI = 3.5.

## Instrumentation

Cyclic voltammograms were recorded on a ALS Electrochemical Analyzer Model 612D with the three electrode system consisting

of a platinum disc working electrode ( $\phi$  = 3 mm), a platinum wire counter electrode, and an Ag/AgCl reference electrode in a acetonitrile containing tetrabutylammonium hexafluorophosphate (0.1 M) at a scan rate of 100 mV s<sup>-1</sup>. Polymer thin films were cast from DCB solutions on the working electrode. All the potentials were calibrated with the half-wave potential of the ferrocene/ferrocenium redox couple measured under identical condition. UV-vis absorption spectra were recorded on a Shimadzu UV-3600 spectrometer. Differential scanning calorimetry (DSC) analysis was carried out with an EXSTAR DSC7020 (SII Nanotechnology, Inc.) at a cooling and heating rate of 10 °C min<sup>-1</sup>. 2D GIXD experiments were conducted at SPring-8 on beamline BL19B2. The samples were irradiated with an X-ray energy of 12.39 keV ( $\lambda$  = 1 Å) at a fixed incident angle of 0.12° through a Huber diffractometer, and the GIXD patterns were recorded on a 2D image detector (Pilatus 300K). The polymer thin films for the GIXD measurement were prepared under the same condition used for the OFET and OPV fabrication as described below. AFM images were obtained with Nanoscope scanning probe microscope system (SII Nanotechnology, Inc.).

## Fabrication and characterization of OFET devices

OFET devices were fabricated in a bottom-gate-top-contact configuration on a heavily doped n<sup>+</sup>-Si(100) wafer with 200 nm-thickness thermally grown SiO<sub>2</sub> ( $C_i$  = 17.3 nF cm<sup>-2</sup>). The Si/SiO<sub>2</sub> substrates were ultrasonicated with water for three min thrice, and acetone and isopropanol for 5 min, respectively, and rinsed in boiled isopropanol for 10 min, and then were subjected to UV-ozone treatment for 30 min. The cleaned substrates were then treated by FDTS as follows. The substrates were left in a Teflon container with several drops of FDTS and then the container was heated to 120 °C for 2 h in the desiccator. The FDTS-treated substrates were ultrasonicated with acetone and isopropanol for 5 min, respectively, and rinsed in boiled isopropanol for 10 min. Polymer thin films were spin-coated from hot DCB solutions (3 g L<sup>-1</sup>) at 1000 rpm for 10 s and then 2500 rpm for 35 s. The polymer films were annealed at 150 °C for 30 min under nitrogen. On top of the polymer thin films, gold drain and source contact electrodes (thickness: 80 nm) with the channel length and width of 40  $\mu$ m and 1500  $\mu$ m, respectively, were deposited using a vacuum evaporator. Current–voltage characteristics of the OFET devices were measured at room temperature under ambient conditions (relative humidity: 30–40%) with a Keithley 4200-SCS semiconductor parameter analyzer. Threshold voltages of the devices were estimated from the transfer plots by extrapolating the square root of the drain current to the horizontal axis. The field-effect mobilities were extracted from the square root of the drain current in the saturation regime ( $V_D$  (source–drain current) = –60 V) by using the following equation,

$$I_D = (WC_i/2L)\mu(V_G - V_T)^2$$

where  $L$  and  $W$  are channel length and width, respectively,  $C_i$  is the capacitance of the SiO<sub>2</sub> gate dielectric,  $I_D$  is the source–drain current, and  $V_G$ , and  $V_T$  are the gate, and threshold voltages,

respectively. The mobilities and threshold voltages were obtained over more than 10 devices.

### Fabrication and characterization of OPV devices

ITO substrates were pre-cleaned sequentially by sonicating in a detergent bath, de-ionized water, acetone, and isopropanol at rt, and in a boiled isopropanol bath, each for 10 min. Then, the substrates were subjected to UV/ozone treatment at rt for 20 min. The ITO substrates masked at the electrical contacts were coated with ZnO precursor by spin coating (3000 rpm for 30 s) a precursor solution prepared by dissolving zinc acetate dehydrate (0.5 g) and ethanolamine (0.14 mL) in 5 mL of 2-methoxyethanol. They were then baked in air at 200 °C for 30 min, then rinsed with acetone and isopropanol, and dried in a glove box. The active layer was deposited in a glove box by spin coating hot (100 °C) DCB solution containing the polymer and PC<sub>71</sub>BM with the weight ratio of 1 : 2 at 600 rpm for 20 s. MoO<sub>x</sub> (7.5 nm) and Ag (100 nm) were deposited sequentially by thermal evaporation under  $\sim 10^{-5}$  Pa, where the active area of the cells was 0.16 cm<sup>2</sup>. *J*-*V* characteristics of the devices were measured with a Keithley 2400 source measure unit in nitrogen atmosphere under 1 Sun (AM1.5G) conditions using a solar simulator (SAN-EI Electric, XES-40S1, 1000 W m<sup>-2</sup>). The light intensity for the *J*-*V* measurements was calibrated with a reference PV cell (Konica Minolta AK-100 certified by the National Institute of Advanced Industrial Science and Technology, Japan). More than 10 devices were analysed. EQE spectra were measured with a Spectral Response Measuring System (Soma Optics, Ltd., S-9241).

### Acknowledgements

This work was financially supported by Grants-in-Aid for Scientific Research (No. 24685030) from MEXT, Japan. High-resolution mass spectrometry and elemental analysis was carried out at the Materials Characterization Support Unit in RIKEN, Advanced Technology Support Division. GIXD experiments were performed at the BL19B2 of SPring-8 with the approval of the Japan Synchrotron Radiation Research Institute (JASRI) (Proposal No. 2013B1719).

### References

- H. Klauk, *Organic Electronics II: More Materials and Applications*, Wiley-VCH Verlag GmbH & Co. KGaA, Weinheim, Germany, 2012.
- G. Hadziioannou and G. G. Malliaras, *Semiconducting Polymers, Chemistry, Physics and Engineering*, Wiley-VCH Verlag GmbH & Co. KGaA, Weinheim, Germany, 2007.
- A. Facchetti, *Chem. Mater.*, 2011, **23**, 733–758.
- I. Osaka and R. D. McCullough, *Acc. Chem. Res.*, 2008, **41**, 1202–1214.
- P. M. Beaujuge and J. M. J. Fréchet, *J. Am. Chem. Soc.*, 2011, **133**, 20009–20029.
- S. Setayesh, D. Marsitzky and K. Müllen, *Macromolecules*, 2000, **33**, 2016–2020.
- W. Zhang, J. Smith, R. Hamilton, M. Heeney, J. Kirkpatrick, K. Song, S. E. Watkins, T. Anthopoulos and I. McCulloch, *J. Am. Chem. Soc.*, 2009, **131**, 10814–10815.
- Q. Zheng, B. J. Jung, J. Sun and H. E. Katz, *J. Am. Chem. Soc.*, 2010, **132**, 5394–5404.
- W. Zhang, J. Smith, S. E. Watkins, R. Gysel, M. McGehee, A. Salleo, J. Kirkpatrick, S. Ashraf, T. Anthopoulos and M. Heeney, *J. Am. Chem. Soc.*, 2010, **132**, 11437–11439.
- Y.-C. Chen, C.-Y. Yu, Y.-L. Fan, L.-I. Hung, C.-P. Chen and C. Ting, *Chem. Commun.*, 2010, **46**, 6503–6505.
- R. S. Ashraf, B. C. Schroeder, H. A. Bronstein, Z. Huang, S. Thomas, R. J. Kline, C. J. Brabec, P. Rannou, T. D. Anthopoulos, J. R. Durrant and I. McCulloch, *Adv. Mater.*, 2013, **25**, 2029–2034.
- Z. Fei, R. S. Ashraf, Z. Huang, J. Smith, R. J. Kline, P. D'Angelo, T. D. Anthopoulos, J. R. Durrant, I. McCulloch and M. Heeney, *Chem. Commun.*, 2012, **48**, 2955–2957.
- Y. Li, Y. Wu and B. S. Ong, *Macromolecules*, 2006, **39**, 6521–6527.
- J. Lu, F. Liang, N. Drolet, J. Ding, Y. Tao and R. Movileanu, *Chem. Commun.*, 2008, 5315–5317.
- J.-H. Tsai, C.-C. Chueh, M.-H. Lai, C.-F. Wang, W.-C. Chen, B.-T. Ko and C. Ting, *Macromolecules*, 2009, **42**, 1897–1905.
- J. E. Donaghey, R. S. Ashraf, Y. Kim, Z. G. Huang, C. B. Nielsen, W. Zhang, B. Schroeder, C. R. G. Grenier, C. T. Brown, P. D'Angelo, J. Smith, S. Watkins, K. Song, T. D. Anthopoulos, J. R. Durrant, C. K. Williams and I. McCulloch, *J. Mater. Chem.*, 2011, **21**, 18744–18752.
- C.-A. Tseng, J.-S. Wu, T.-Y. Lin, W.-S. Kao, C.-E. Wu, S.-L. Hsu, Y.-Y. Liao, C.-S. Hsu, H.-Y. Huang, Y.-Z. Hsieh and Y.-J. Cheng, *Chem.-Asian J.*, 2012, **7**, 2102–2110.
- J.-S. Wu, C.-T. Lin, C.-L. Wang, Y.-J. Cheng and C.-S. Hsu, *Chem. Mater.*, 2012, **24**, 2391–2399.
- L. Biniek, B. C. Schroeder, J. E. Donaghey, N. Yaacobi-Gross, R. S. Ashraf, Y. W. Soon, C. B. Nielsen, J. R. Durrant, T. D. Anthopoulos and I. McCulloch, *Macromolecules*, 2013, **46**, 727–735.
- I. McCulloch, R. S. Ashraf, L. Biniek, H. Bronstein, C. Combe, J. E. Donaghey, D. I. James, C. B. Nielsen, B. C. Schroeder and W. Zhang, *Acc. Chem. Res.*, 2012, **45**, 714–722.
- M. M. Wienk, M. Turbiez, J. Gilot and R. A. J. Janssen, *Adv. Mater.*, 2008, **20**, 2556–2560.
- L. Bürgi, M. Turbiez, R. Pfeiffer, F. Bienewald, H.-J. Kirner and C. Winnewisser, *Adv. Mater.*, 2008, **20**, 2217–2224.
- R. Stalder, J. Mei and J. R. Reynolds, *Macromolecules*, 2010, **43**, 8348–8352.
- T. Lei, Y. Cao, Y. Fan, C.-J. Liu, S.-C. Yuan and J. Pei, *J. Am. Chem. Soc.*, 2011, **133**, 6099–6101.
- C. Piliago, T. W. Holcombe, J. D. Douglas, C. H. Woo, P. M. Beaujuge and J. M. J. Fréchet, *J. Am. Chem. Soc.*, 2010, **132**, 7595–7597.
- Y. Zou, A. Najari, P. Berrouard, S. Beaupré, B. R. Aich, Y. Tao and M. Leclerc, *J. Am. Chem. Soc.*, 2010, **132**, 5330–5331.

- 27 J. A. Letizia, M. R. Salata, C. M. Tribout, A. Facchetti, M. A. Ratner and T. J. Marks, *J. Am. Chem. Soc.*, 2008, **130**, 9679–9694.
- 28 X. Guo, N. Zhou, S. J. Lou, J. Smith, D. B. Tice, J. W. Hennek, R. P. Ortiz, J. T. L. Navarrete, S. Li, J. Strzalka, L. X. Chen, R. P. H. Chang, A. Facchetti and T. J. Marks, *Nat. Photonics*, 2013, **7**, 825–833.
- 29 Z. Chen, Y. Zheng, H. Yan and A. Facchetti, *J. Am. Chem. Soc.*, 2009, **131**, 8–9.
- 30 X. Guo and M. D. Watson, *Org. Lett.*, 2008, **10**, 5333–5336.
- 31 H. Yan, Z. Chen, Y. Zheng, C. Newman, J. R. Quinn, F. Dötz, M. Kastler and A. Facchetti, *Nature*, 2009, **457**, 679–686.
- 32 I. Osaka, M. Akita, T. Koganezawa and K. Takimiya, *Chem. Mater.*, 2012, **24**, 1235–1243.
- 33 M. K. Poduval, P. M. Burrezo, J. Casado, J. T. López Navarrete, R. P. Ortiz and T.-H. Kim, *Macromolecules*, 2013, **46**, 9220–9230.
- 34 J. Cao, Q. Liao, X. Du, J. Chen, Z. Xiao, Q. Zuo and L. Ding, *Energy Environ. Sci.*, 2013, **6**, 3224–3228.
- 35 H. Huang, Z. Chen, R. P. Ortiz, C. Newman, H. Usta, S. Lou, J. Youn, Y.-Y. Noh, K.-J. Baeg, L. X. Chen, A. Facchetti and T. Marks, *J. Am. Chem. Soc.*, 2012, **134**, 10966–10973.
- 36 R. Kroon, A. Diaz de Zerio Mendaza, S. Himmelberger, J. Bergqvist, O. Bäcke, G. C. Faria, F. Gao, A. Obaid, W. Zhuang, D. Gedefaw, E. Olsson, O. Inganäs, A. Salleo, C. Müller and M. R. Andersson, *J. Am. Chem. Soc.*, 2015, **137**, 550.
- 37 K. Kawabata, I. Osaka, M. Nakano, N. Takemura, T. Koganezawa and K. Takimiya, *Adv. Electron. Mater.*, 2015, **1**, 1500039.
- 38 I. Osaka, M. Saito, T. Koganezawa and K. Takimiya, *Adv. Mater.*, 2014, **26**, 331–338.
- 39 K. Takimiya, I. Osaka and M. Nakano, *Chem. Mater.*, 2013, **26**, 587–593.
- 40 L. Huo, T. Liu, X. Sun, Y. Cai, A. J. Heeger and Y. Sun, *Adv. Mater.*, 2015, **27**, 2938–2944.
- 41 L. Huo, T. Liu, B. Fan, Z. Zhao, X. Sun, D. Wei, M. Yu, Y. Liu and Y. Sun, *Adv. Mater.*, 2015, **27**, 6969–6975.
- 42 J. J. S. Lamba and J. M. Tour, *J. Am. Chem. Soc.*, 1994, **116**, 11723–11736.